ELSEVIER

Gene 228 (1999) 197–211

GENE
AN INTERNATIONAL JOURNAL ON GENES AND GENOMES

Identification of ZFR, an ancient and highly conserved murine chromosome-associated zinc finger protein

Madeleine J. Meagher [a], Jill M. Schumacher [a,1], Keesook Lee [a,2], Robert W. Holdcraft [a], Susanne Edelhoff [b], Christine Disteche [b], Robert E. Braun [a,*]

[a] *Department of Genetics, University of Washington, Seattle, WA 98195, USA*
[b] *Department of Pathology, Box 357470, University of Washington, Seattle, WA 98195, USA*

Received 10 June 1998; received in revised form 30 November 1998; accepted 30 November 1998; Received by C.M. Kane

Abstract

In a screen for RNA binding proteins expressed during murine spermatogenesis, we cloned a novel, ancient zinc finger protein possessing a region common to a small class of RNA binding proteins. *Zfr* (zinc finger RNA binding) encodes a protein of 1052 amino acids with three widely spaced Cys_2His_2 zinc fingers. Outside of the zinc fingers, ZFR shares a region that is highly conserved between several RNA binding proteins containing copies of the double-stranded RNA binding motif. By northern blotting, *Zfr* is expressed at highest levels within the testis, ovary and brain. Immunohistochemistry and confocal microscopy were used to show that ZFR is highly expressed during meiosis I in males and females and is chromosome associated. *Zfr* is also expressed in Sertoli cells in the testis and granulosa cells in the ovary where it is localized to the nucleus. Using fluorescent in situ hybridization we mapped *Zfr* to chromosome 15 region A. ZFR appears to be an ancient protein, as apparent homologs exist in invertebrates (*D. melanogaster*) nematodes (*C. elegans*) and humans (*H. sapiens*).

Keywords: Meiosis; Ovary; Post-transcriptional; Testis

1. Introduction

Spermatogenesis encompasses a unique set of differentiation steps and morphogenetic changes. The program includes the commitment of a proliferating stem germ cell to terminal differentiation, the process of meiosis, and unique morphological restructuring to form the highly specialized spermatozoon. The identification of regulatory proteins that operate during spermatogenesis is of interest as they underlie the execution of these diverse yet linked developmental programs.

As in other developmental pathways, germ cell differentiation is likely to be promoted at the transcriptional level by testis-expressed transcription factors. A major class of growth and development regulatory proteins are the zinc finger motif-containing proteins. Several testis-expressed zinc finger proteins have been identified, in some cases from screens of testis cDNA

* Corresponding author. Tel.: +1-206-543-1818; fax: +1206-543-0754; e-mail: braun@genetics.washington.edu.
[1] ABL-Basic Research Program, NCI-FCRDC, Frederick, MD 21702, USA.
[2] Hormone Research Center, Chonnam National University, Kwangju 500-757, South Korea.

Abbreviations: BLAST, basic local alignment search tool; bp, base pair(s); cDNA, DNA complementary to RNA; DABCO, 2.5% 14-diazobicyclo-[2.2.2]-octane; DAPI, 4'6-diamidino-2-phenylindole; dsRBM, double-stranded RNA binding motif; dsRBP-ZFa, double-stranded RNA binding protein zinc finger a protein; dsRNA, double-stranded RNA; EST, expressed sequence tag; FAR, finger associated repeats; FISH, fluorescence in situ hybridization; FOG, friend ofGATA-1 protein; GAL4, galactose 4 protein; hnRNP, heterogeneous nuclear ribonucleoprotein; hGH, human growth hormone; Ig, immunoglobulin; IPTG, isopropyl β-D-thiogalactopyranoside; kb, kilobase(s); kDa, kilodalton(s); MBP, maltose binding protein; μg, microgram; NCBI, National Center for Biotechnology Information; NF45, nuclear factor 45 protein; NF90 nuclear factor 90 protein; NLS, nuclear localization signal; PAGE, polyacrylamide gel electrophoresis; PBS, phosphate buffered saline; PEP, protein on ecdysone perinuclear RNA binding protein; TFIIIA, transcription factor IIIA protein; UTR, untranslated region; *Zfr*, gene encoding zinc finger RNA binding protein; YAC, yeast artificial chromosome.

0378-1119/99/$ – see front matter
PII: S0378-1119(98)00615-5

libraries probed with the highly conserved interfinger linker residues.

The first identified zinc finger protein, *Xenopus* TFIIIA, functions in both a DNA and RNA binding capacity (Klug and Rhodes, 1987). In frog oocytes the TFIIIA protein binds a DNA site for the transcriptional regulation of the 5S DNA genes and, additionally, binds the nascent 5S rRNA for storage and transport. Subsequent to the initial description in TFIIIA, zinc finger motifs have been identified in a large number of nucleic acid binding proteins. The majority of zinc finger proteins are considered to function as DNA-binding proteins, although a few proteins have a demonstrated preference for RNA molecules as substrates.

Reported here is the discovery of a novel, ancient zinc finger protein from a screen designed to identify RNA-binding proteins expressed during murine spermatogenesis. A screen of a testis cDNA expression library with radiolabeled RNA identified five new genes. Four of these, *Spnr* (Schumacher et al., 1995b), *Tenr* (Schumacher et al., 1995a), *Prbp* (Lee et al., 1996), and the mouse homolog of *NF90* (unpublished observation), encode proteins containing copies of the double-stranded RNA binding motif (dsRBM). A fifth gene, described here, encodes a novel protein containing three, widely spaced Cys_2His_2 zinc finger motifs and a 314 amino acid domain that is highly conserved in a small number of dsRBM-containing proteins including SPNR and mouse NF90.

2. Materials and methods

2.1. Cloning and sequencing of Zfr cDNAs

λgt11 cDNA expression libraries prepared from RNA from round spermatids or from pachytene spermatocytes were screened with *Prm1* or *hGH* RNA as described previously (Schumacher et al., 1995b). To obtain additional *Zfr* cDNAs, the pachytene spermatocyte library was plated and screened with a 250 bp fragment from the 5′ end of cDNA *Zfr.2*. A testis cDNA bacterial library (Clonetech, Palo Alto, CA) was plated and screened with a 242 bp fragment from the 5′ end of cDNA *Zfr.3*. The cDNAs *Zfr.3* and *Zfr.4* were subcloned into the Bluescript vector pKS (Stratagene, La Jolla, CA). A composite cDNA was cloned by fusing the 5′ end of *Zfr.3* with the 3′ end of *Zfr.1* at a unique Nsi I site. Templates for sequencing were generated by subcloning and by exonuclease III deletion (Sambrook et al., 1989). Sequencing was performed using ^{35}S and Sequenase kits (USB, Cleveland, OH) and using Dye-terminator cycle sequencing kits (Perkin Elmer, Norwalk, CN). Database analyses and searches were performed using the SAPS and BLAST Internet servers.

2.2. Fluorescence in situ hybridization

A probe containing a 2.6 kb insert of *Zfr* cDNA was labeled with biotin-11-dUTP by nick translation (Gibco BRL, Gaithersburg, MD). The size of the product was determined to be between 200 and 400 bp. Metaphase chromosome preparations from lymphocytes of a male C57BL/6J mouse were obtained using 0.075 M KCL as a hypotonic buffer and methanol:acetic acid (3:1, v/v) as fixative. The hybridization was carried out as previously described (Edelhoff et al., 1994). Hybridization signals were detected using a detection system from Vector (Burlingame, CA). After incubation with goat anti-biotin antibody, slides were rinsed in modified PBS (0.2 M NaH_2PO_4, 0.15 M Na_2HPO_4, 0.15 M NaCl, 0.1% Tween 20, and 0.15% bovine serum albumin). A second incubation with fluorescein-labeled anti-goat IgG and a rinse in modified PBS followed. The chromosomes were banded using Hoechst 33258-actinomycin D staining and counterstained with propidium iodide. The chromosomes and hybridization signals were visualized by fluorescence microscopy, using a dual band pass filter (Omega or Chroma, Brattleboro, VT).

2.3. Maltose binding protein fusion protein expression and antibody production

The 1.3 kb HindIII fragment from the *Zfr.1* cDNA was cloned in frame into the pMAL-c2 expression vector (NEB, Beverly, MA). A maltose-binding-protein-ZFR fusion protein was induced from transformed DH5α *E. coli* cells with IPTG and affinity purified from the cell lysate on an amylose resin column as described by NEB. Injection of MBP-ZFR into rabbits to raise antiserum was performed by R&R Rabittry (Stanwood, WA). Anti-MBP-ZFR antibodies were affinity purified by incubating the sera from the sixth bleed with fusion protein bound to either a nitrocellulose filter or a cyanogen bromide-activated Sephadex bead column (Sambrook et al., 1989).

2.4. Immunohistochemistry and immunofluorescence

Testes and ovaries from 6–8 week old adult mice were dissected, fixed in Carnoy's and embedded in paraffin. For immunohistochemistry, tissue sections were incubated with anti-ZFR antibodies diluted 1:1000 in 3% goat serum and treated with biotinylated goat anti-rabbit IgG followed by streptavidin-horse radish peroxidase conjugate. Antigen was visualized using 3-amino-9-ethylcarbazole as the chromogenic substrate for peroxidase (Vector Laboratories, Burlingame, CA). Sections were counterstained briefly with hematoxylin and mounted. For immunofluorescence, sections were incubated with anti-ZFR antibodies diluted 1:500 in 3% goat serum, treated with fluorescein-conjugated goat

anti-rabbit IgG (Zymed Laboratories, South San Francisco, CA) and briefly counterstained with 4′6-diamidino-2-phenylindole (DAPI). Sections were mounted in 90% glycerol with 2.5% 1,4-diazobicyclo-[2.2.2]-octane (DABCO) and subjected to confocal microscopy.

2.5. Spread spermatocyte preparation and immunofluorescence

Spermatocyte spreads were prepared according to the methods described by Haaf et al. (1989). Briefly, a cell suspension was prepared from mouse testes, the cell density was adjusted to 10^5 cells/ml, and attached to slides by cytocentrifugation. The cells were incubated with PBS containing Triton-X and DTT to spread the chromosomes. Cells were fixed in methanol and acetone. The spread spermatocytes were co-incubated with anti-ZFR antibodies and the human serum, treated with Texas red-conjugated anti-human IgG and fluorescein-conjugated anti-rabbit IgG, mounted and imaged by confocal microscopy.

2.6. Protein preparation and western blot analysis

Sertoli cell line 15P-1 was obtained from D. Wolgemuth. Protein from 15P-1 cells and from adult mouse testes was isolated and separated into nuclear and cytoplasmic fractions by centrifugation. 50 μg of protein from each fraction were electrophoresed, western blotted, and visualized by chemiluminescence according to described protocols (Sambrook et al., 1989). To preabsorb anti-ZFR antibodies, 30 μg of MBP-ZFR fusion protein was preincubated with the antibody preparation at 4°C for 5 h prior to the primary antibody incubation step in the western blot procedure. In vitro translation products were generated using the composite *Zfr* cDNA and the TNT coupled transcription/translation reticulocyte lysate system (Promega, Madison, WI). The product was visualized by ^{35}S-methionine autoradiography and by western blot analysis.

2.7. RNA preparation and northern blot analysis

RNA from adult mouse tissues was extracted by homogenization in guanidinium isothiocyanate and precipitation with lithium chloride. 10 μg of RNA from each sample was electrophoresed in a 1.5% formaldehyde agarose gel, blotted to nitrocellulose, and probed with *Zfr.1* cDNA sequence. The blot was reprobed with a 114 bp HindIII–BamHI DNA fragment from murine adult skeletal alpha-actin.

2.8. Histidine-tagged fusion protein expression and nucleic acid binding assays

To obtain bacterially expressed histidine-tagged ZFR protein, cDNA *Zfr.1* was cloned in frame into the NdeI site in the pET15b plasmid (Novagen, Madison WI). BL21 (DE3) bacterial cells were transformed with either pET15b vector or pET15b-*Zfr.1*. Cultures of 25 ml for each strain were induced with 1 mM IPTG for 3 h. 0.25 ml samples of crude cell extracts were separated by SDS–polyacrylamide gel electrophoresis and transferred to Immobilon-P PVDF membrane (Millipore, Bedford, MA). A fraction of each blot was used for western blotting with anti-His antibody. The binding assays were performed as described previously (St Johnston et al., 1992). The remainder of the blots were denatured in 8 M urea and slowly renatured via ten 2:3 step dilutions with Tris-buffered saline. Membranes were blocked in 25 mM NaCl, 10 mM $MgCl_2$, 10 mM Hepes pH 8, 0.1 mM EDTA, 1 mM dithiothreitol, and 5% non-fat dry milk. Probes were incubated with the blot in 50 mM NaCl, 10 mM $MgCl_2$, 10 mM Hepes pH 8, 0.1 mM EDTA, 1 mM dithiothreitol, and 2.5% non-fat dry milk. Radiolabeled ssRNA was produced by SP6 in vitro transcription of the *Prm1* 3′ untranslated sequence. The VA RNA_I gene was transcribed in vitro using T7 DNA polymerase. Both reactions were subsequently treated with RNase-free DNase (Promega, Madison WI). The synthesis and integrity of the RNAs were ascertained by scintillation counting of TCA-precipitated samples and by native 5% PAGE. The *Prm1* RNA was heated to 85°C for 5 min and added to the blot at 10^7 cpm/ml. The VA RNA_I was heated to 65°C for 10 min, then slowly cooled to room temperature to generate the structured conformation and added to the blot at 2.5×10^6 cpm/ml. DNA probes were obtained by random hexanucleotide-primed DNA synthesis from the first 1200 bp of cDNA sequence from the *Spnr* gene. Probes were purified using Centrisep columns (Princeton Separations, Princeton, NJ). A fraction of the reaction was boiled for 5 min for denaturation. Denatured and undenatured DNA probe samples were incubated with blots at concentrations of 2.5×10^6 cpm/ml. All blots were washed in the binding buffer three times for 10 min at room temperature and exposed to X-ray film for 3 h.

3. Results

3.1. Molecular screen for RNA binding proteins

RNAs encoding many of the sperm structural proteins, including the protamines, are synthesized in meiotic or early post-meiotic cells, translationally repressed for several days, and translated in late-stage spermatids. Translational repression of the protamine 1 mRNA

(*Prm1*) is required for normal spermatogenesis and is mediated by sequences in its 3′ untranslated region (3′UTR). In an effort to clone murine RNA binding proteins that potentially function in protamine translational control, λgt11 cDNA expression libraries constructed from RNA from pachytene spermatocytes or round spermatids were screened with an RNA probe transcribed from the 3′UTR of *Prm1*. To minimize the likelihood of choosing clones that nonspecifically bound RNA, the filters were rescreened with an RNA probe transcribed from the 3′UTR of human growth hormone (*hGH*), a gene whose 3′UTR does not confer translational delay (Braun et al., 1989). 19 clones, representing five genes, exhibited preference for the *Prm1* probe (Schumacher et al., 1995a,b; Lee et al., 1996). Two cDNAs for a gene we refer to as *Zfr* (zinc finger RNA binding) were isolated, one from the pachytene spermatocyte library and one from the round spermatid library.

The *Zfr* cDNAs (Fig. 1) were sequenced from plasmid subclones and exonuclease III deletion clones. An open reading frame incomplete at the 5′ end was found in the overlapping *Zfr.1* and *Zfr.2* cDNA sequences. Additional 5′ cDNA clones were isolated by screening the λgt11 pachytene spermatocyte cDNA library and a testis cDNA plasmid library. cDNAs *Zfr.3* and *Zfr.4* carry the same in-frame translational stop near the 5′ end of the sequence, suggesting that the large open reading frame downstream is complete. To construct a composite cDNA with a full-length open reading frame, the 5′ portion of cDNA *Zfr.3* was fused with the 3′ portion of cDNA *Zfr.1* at a unique Nsi I site. In vitro transcription and translation of this sequence demonstrated that this cDNA encodes the full-length protein (see Section 3.6).

Overlapping regions of the cDNAs share identical nucleotide sequence with one exception. *Zfr.2* contains a 98 bp internal deletion corresponding to positions 2748–2845 in the composite sequence. This deletion could have arisen from a reverse transcriptase error in the cDNA library preparation. Alternatively, *Zfr.2* may represent an alternatively spliced *Zfr* transcript (see below). An additional 3′ *Zfr* cDNA cloned by 3′ RACE (data not shown) was found to contain the DNA deleted in *Zfr.2* and perfectly match the 3′ nucleotide sequence in *Zfr.1*.

Two putative translation initiation methionine codons were found immediately downstream from the in-frame stop. According to the consensus for the nucleotide context of initiation sites, a guanine is the favored nucleotide at position +4, and a purine, most commonly adenine, is almost invariably found at position −3. Nonfunctional AUGs, in contrast, often have a pyrimidine at position −3. The first AUG in the *Zfr* open reading frame is in poor context for initiation (CCCAUGA). The sequence at the second AUG conforms to the consensus at the −3 and +4 positions (AAAAUGG). Translation of *Zfr* therefore most likely initiates from the second methionine.

The *Zfr* cDNA coding sequence is preceded by a 174 bp 5′ untranslated sequence that is most likely incomplete based on the size of the *Zfr* transcript (see Section 3.5). A 3′ untranslated sequence of 326 bp follows the coding sequence and ends with a tract of 40 adenosines. The 3′UTR lacks the canonical polyadenylation signal, AATAAA, and instead contains the most common functional variant, ATTAAA. This sequence is situated at a typical distance of 20 bp from the start of the poly(A) tail.

3.2. ZFR is a zinc finger protein

Sequencing of the *Zfr* cDNAs revealed that ZFR is a novel, conserved protein containing three copies of the C_2H_2 zinc finger motif (Fig. 2). All three fingers can be described by the consensus $CX_2CX_{12}HX_5H$. The zinc finger motifs are notably widely spaced from each other; fingers 1 and 2 are separated by 27 amino acids and fingers 2 and 3 are separated by 177 amino acids.

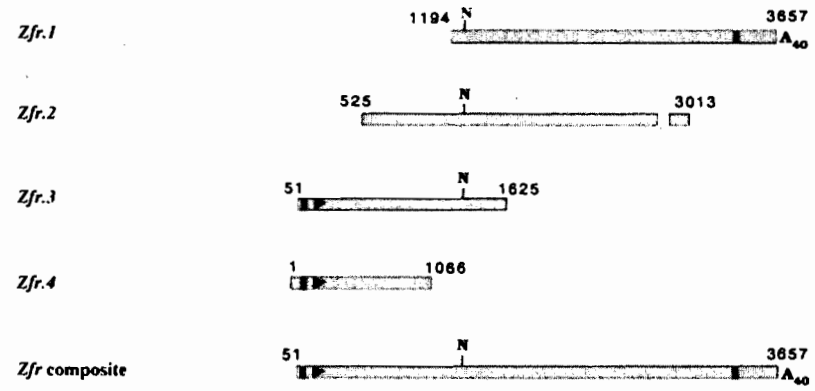

Fig. 1. Schematic of four *Zfr* cDNAs and a composite *Zfr* cDNA. The numbers adjacent to the boxes denote the nucleic acid numbering. The arrow represents the second ATG in the sequence, encoding the probable translation initiation site. The black squares represent in-frame translational stops. In *Zfr.2*, bases 2748–2845 are deleted. The unique Nsi I site was used to construct the *Zfr* composite cDNA from *Zfr.3* and *Zfr.1*.

```
MATGNYFGFT HSGAAAAAAA AQYSQQPASG VAYSHPTTVA SYTVHQAPVA AHTVTAAYAP      60
AAATVAVARP APVAVAAAAT AAAYGGYPTA HTATDYGYTQ RQQEAPPPPP PATTQNYQDS     120
YSYVRSTAPA VAYDSKQYYQ QPTATAAAVA AAAQPQPSVA ETYYQTAPKA GYSQGATQYT     180
QAQQARQVTA IKPATPSPAT TTFSIYPVSS TVQPVAAAAT VVPSYTQSAT YSTTAVTYSG     240
TSYSGYEAAV YSAASSYYQQ QQQQQKQAAA AAAAAAATAA WTGTTFTKKT PFQNKQLKPK     300
QPPKPPQIHY CDVCKISCAG PQTYKEHLEG QKHKKKEAAL KASQNTSSSN NSTRGTQNQL     360
RCELCDVSCT GADAYAAHIR GAKHQKVVKL HTKLGKPIPS TEPNVVSQAT SSTAASASKP     420
TASPSSIGAS NCTLNTSSIA TSSVKGLSTT GNSSLNSTSN TKVSAIPTNM AAKKTSTPKI     480
NFVGGNKLQS TGNKTEDLKG IDCVKNTPAA SAVQIPEVKQ DAGSEPVTPA SLAALQSDVQ     540
PVGHDYVEEV RNDEGKVIRF HCKLCECSFN DPNAKEMHLK GRRHRLQYKK KVNPDLQVEV     600
KPSIRARKIQ EEKMRKQMQK EEYWRRREEE ERWRMEIRRY EEDMYWRRME EEQHHWDDRR     660
RMPDGGYPHG PPGPLGLLGV RPGMPPQPQG PAPLRRPDSS DDRYVMTKHA TIYPTEEELQ     720
AVQKIVSITE RALKLVSDSL SEHEKSKNKE GDDKKEGGKD RALKGVLRVG VLAKGLLLRG     780
DRNVNLVLLC SEKPSKSLLS RIAENLPKQL AVISPEKYDI KCAVSEAAII LNSCVEPKMQ     840
VTITLTSPII REENMREGDV TSGMVKDPPD VLDRQKCLDA LAALRHAKWF QARANGLQSC     900
VIIIRILRDL CQRVPTWSDF PSWAMELLVE KAISSASSPQ SPGDALRRVF ECISSGIILK     960
GSPGLLDPCE KDPFDTLATM TDQOREDITS SAQKALRLLA FRQIHKVLGM DPLPQMNQRF    1020
NIHNNRKRRR DSDGVDGFEA EGKKDKKDYD NF
1052
```

Fig. 2. Predicted amino acid sequence for ZFR. Double-underlined sections are the zinc fingers; single-underlined sections are the ZRA1 and ZRA2 regions. Dotted regions are putative bipartite nuclear localization signals. Homopolymeric stretches of alanine (14–21; 268–280) and glutamine (259–265) lie upstream of the zinc fingers. A glycine/proline-rich region (665–693) precedes the ZRA regions. Regions with mixed positive and negative charge are downstream of the third finger, at the junction between ZRA1 and ZRA2, and at the second putative NLS (amino acids 611–661, 742–761, and 1026–1048 respectively). The GenBank accession number is AF071059.

The conserved seven amino acid sequence that typically links tandem finger motifs is thus absent in *Zfr*. The structure of each finger conforms generally to the classical C_2H_2 consensus originally created from the analysis of the zinc-binding motifs in *Xenopus* TFIIIA (Klug and Rhodes, 1987), but is most similar to the fingers found in the *Xenopus* double-stranded RNA binding protein dsRBP-ZFa (Finerty and Bass, 1997). All three fingers have a moderately long interhistidine distance of five amino acids. Within the 12 residue stretch between the cysteines and histidines, zinc fingers generally possess a conserved aromatic residue at the fourth position (+4) and a hydrophobic residue at the tenth position (+10). The first two fingers of ZFR show a reversal in the placement of these residues with a cysteine at +4 and a tyrosine at +10. The third finger has a canonical phenylalanine at +4 but substitutes the hydrophobic residue at +10 with lysine.

The carboxy-terminal third of the protein shares a high degree of similarity with a collection of double-stranded RNA binding motif-containing proteins (Fig. 3A, light gray box). Database searches using local alignment search programs (BLAST) revealed an amino acid identity, ranging from 57% to 65%, between the carboxy-terminal half of ZFR with the amino-terminal half of the murine spermatid perinuclear RNA binding protein (SPNR), *Xenopus* dsRNA binding proteins 4F.1 and 4F.2, and human nuclear factor of activated T-cells (NF-AT) complex protein NF90 (Fig. 3A and B). SPNR, NF90, and 4F.1 align with two regions in ZFR that are separated by a short tract of more divergent sequence. A weaker alignment to the second region was also found with human NF-AT complex protein NF45. Downstream from the regions of alignment with ZFR, these proteins, with the exception of NF45, bear two copies of the double-stranded RNA binding motif (dsRBM) (St Johnston et al., 1992). The conserved regions, here referred to as ZRA1 and ZRA2 (for zinc finger motif and RNA binding motif-associated) contain no previously characterized protein motifs.

Flanking ZRA1 and ZRA2 are two putative nuclear localization signals (NLS). The first site at amino acid positions 647–663 matches the consensus for the bipartite nuclear localization motif in which two basic residues are followed by a ten amino acid spacer and a five amino acid stretch containing three basic residues (Robbins et al., 1991). A second sequence at positions 1026–1047 also matches this pattern but contains a

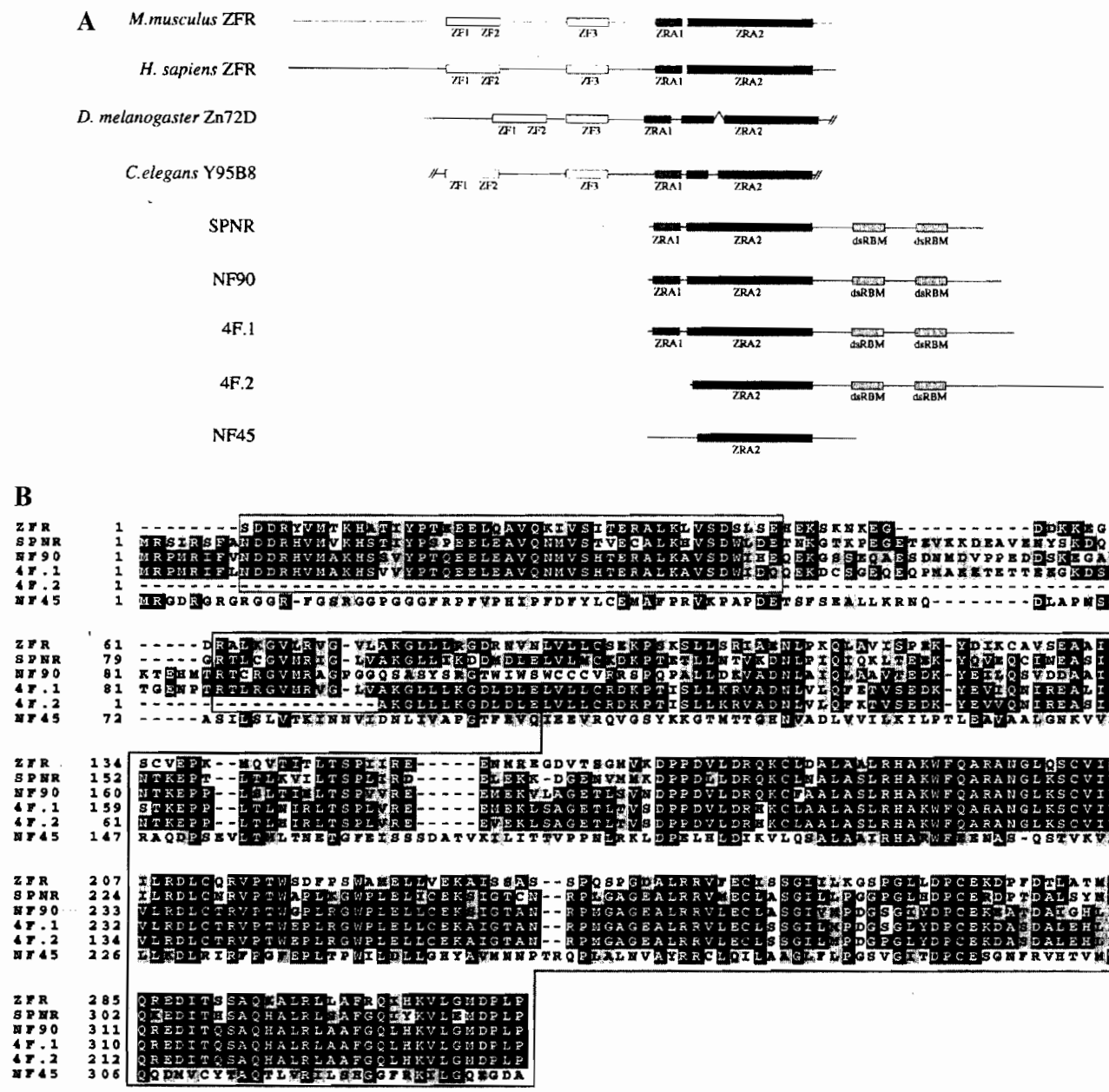

Fig. 3. (A) Schematic alignment of the murine ZFR protein with other proteins containing the highly conserved ZRA regions, and with human, *Drosophila* and *C. elegans* homologs. The *Xenopus* 4F.1, murine SPNR, and human NF90 proteins begin with a ZRA1 region (dark gray box) and a ZRA2 region (black bar) whereas *Xenopus* 4F.2 starts in the ZRA2 region. Two copies of the dsRNA binding motif (light gray boxes) follow. Human protein NF45 has a weaker alignment to ZRA2. Murine ZFR and human ZFR are homologous throughout the protein. *Drosophila* Zn72D and the *C. elegans* homolog share similarity with murine ZFR at the zinc finger regions (indicated) and the ZRA regions. Zn72D contains a 67 amino acid insertion within ZRA2 that does not align with ZFR. The size of the nematode protein, and the spacing of its motifs, have not yet been established. (B) Amino acid alignment of the ZRA1 (first box) and ZRA2 (second box) regions from ZFR, SPNR, NF90, 4F.1, 4F.2, and NF45. Identical amino acids are shaded black; conservative amino acid changes are shaded gray. The initial N-terminal residues are shown for SPNR, NF90, 4F.1, and NF45 to orient the location of the ZRA regions within the sequences. The more divergent NF45 protein has an organization generally similar to the other proteins but has significant amino acid matches only within the ZRA2 region.

spacer of 12 residues. Spacer lengths larger than ten residues are common and still allow efficient nuclear targeting (Robbins et al., 1991). Nuclear targeting of ZFR might be accomplished by the independent function of one of these sequences or by the additive function of both signals.

The 1052 amino acid sequence encodes a basic protein with a predicted p*I* of 9.19. Analysis of the amino acid sequence using the Statistical Analysis of Protein Sequences (SAPS) program revealed that the ZFR contains three regions of mixed negative and positive charge (Brendel et al., 1992). The third zinc finger is followed

by an arginine- and glutamic acid-rich stretch, and the carboxy terminal residues at the second NLS are rich in lysine, glycine, arginine, and glutamic acid (Fig. 2). The sequence that joins the ZRA1 and ZRA2 regions is glycine-rich and has a mixed charge due to lysine and glutamic acid residues. The amino-terminal start of the protein, in contrast, is uncharged and contains homopolymeric stretches of alanine and glutamine. A span of glycines and prolines at amino acids 665–693, just upstream of ZRA1, may serve as a flexible linker region between different functional domains.

3.3. *A ZFR protein exists in worms, flies and humans*

DNA and protein sequence searches revealed that homologs of *Zfr* have been cloned from invertebrates and vertebrates. A *D. melanogaster* protein, Zn72D, shares a remarkably similar organization with ZFR (Fig. 3A). High percentages of amino acid conservation can be found in the three zinc fingers and the ZRA regions. Within the first zinc finger, ZFR and Zn72D share 29 of the 34 residues. The remaining five residues are conservative amino acid substitutions. Likewise, the second and third fingers are almost completely conserved between species. Throughout the ZRA regions downstream of the zinc fingers, with the exception of a 67 amino acid insertion in Zn72D, the murine and *Drosophila* proteins share 60% amino acid identity and 74% amino acid similarity. The nature of the insertion in Zn72D, as well as the true translational stop in the open reading frame (Fig. 3A), is uncertain owing to frameshifts in the open reading frame of the GenBank sequence.

A preliminary search of the *C. elegans* genomic sequence databases with the ZFR peptide sequence produced a match with an unnamed gene in YAC Y95B8 on chromosome I. The regions of evolutionary conservation between the worm protein and ZFR are analogous to those seen with the fly protein (Fig. 3A). Amino acid percentages of 49–55% identity and 63–68% similarity were found in the zinc finger regions. A weaker but consistent alignment, exhibiting approximately 34% amino acid identity and 55% similarity, was found in the ZRA1 and ZRA2 regions in the carboxy terminus.

Translations of *Zfr*-like sequences found in the NCBI human Expressed Sequence Tags (EST) database generally display 90–99% amino acid identity to mouse ZFR throughout the protein (Fig. 3A). The amino-terminal sequence in human ZFR is best represented by a cDNA identified in a molecular screen for CAC/GTG repeat-containing genes (Epplen and Epplen, 1994). Its uninterrupted, almost perfect match to mouse ZFR, from the start of the open reading frame to the third zinc finger, demonstrates that the residues between the zinc finger motifs have been highly conserved in recent evolution.

The co-conservation of the three zinc fingers with the novel downstream domain in invertebrates to humans suggests that *Zfr* is an ancient gene functioning in an important process common to these organisms. The sequence alignments show conservation of amino acids flanking the zinc finger motifs, suggesting that these residues might be important for zinc finger structure or target interactions.

3.4. *Mapping of* Zfr

The *Zfr* gene was mapped by fluorescent in situ hybridization (FISH) to the proximal tip of mouse chromosome 15. Of 30 cells examined, 14 (47%) showed signals on both chromatids of one or both chromosomes 15 at region A (Fig. 4). There was no significant hybridization to other chromosomes, suggesting that *Zfr* is a single copy gene.

3.5. Zfr *transcripts*

To investigate the RNA expression profile for *Zfr*, northern blot analyses were performed. A band of 5.0 kb was most strongly detected in the testis and brain (Fig. 5). A second band of 3.9 kb, consistently strong in the testis and weak in the brain, and a third band of 1.7 kb were also observed. Moderate levels of the 5.0 kb and the 3.9 kb species were also detected in the ovary. Longer exposures revealed that both species are expressed at low levels in the heart, kidney, liver, and spleen. Similar results were found from an RNase protection experiment, in which tissue RNA samples were assayed for the ability to protect labeled *Zfr* RNA probes from RNase I degradation (data not shown). The difference in the size of the largest *Zfr* transcript, the 5.0 kb transcript, and the composite *Zfr* cDNA is presumably due to additional 5′ or 3′ untranslated sequence. The 3.9 and 1.7 kb transcripts detected may be alternatively spliced forms of *Zfr* and are not cross-hybridizing *Spnr* or *NF90* RNAs. Northern blots probed with *Spnr* and *NF90* detect a different collection of transcripts than those observed here (data not shown). The high levels of RNA expression in the testis correlate with the immunohistochemistry observations (Section 3.7). The varying abundance of *Zfr* RNA among different tissues and the detection of multiple RNA species suggest that *Zfr* is a differentially expressed gene, and that alternative RNA processing may be an important aspect of its regulation and function.

3.6. *Detection of ZFR protein by western blot*

To raise anti-ZFR antibodies for western blot analysis and immunohistochemistry experiments, a fusion protein between maltose-binding-protein (MBP) and ZFR was expressed in bacteria and injected into rabbits. Anti-

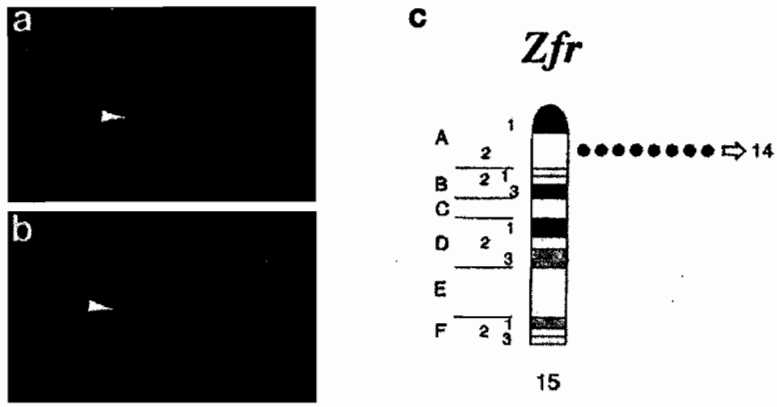

Fig. 4. FISH mapping of the *Zfr* gene. (a) Signals on chromosome 15. (b) Identification of chromosome 15 by banding. (c) A partial map of mouse chromosome 15. Map banding regions are indicated on the left. The map position of *Zfr* is indicated by the dotted line representing 14 signals of hybridization.

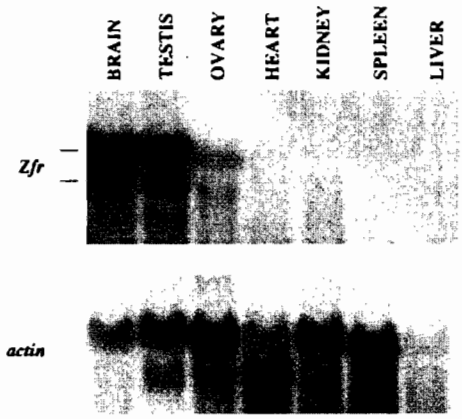

Fig. 5. Northern blot with total RNA from mouse tissues. Radiolabeled *Zfr* DNA probe (top panel) detects *Zfr* transcripts of 5.0 and 3.7 kb in the brain, testis, and ovary. Both bands are weakly present in the remaining tissues in longer exposures. The blot was reprobed with actin (lower panel).

ZFR antibodies were affinity purified and tested on western blots containing nuclear and cytoplasmic extracts prepared from mouse testes. Fractionated extracts were also prepared from a Sertoli cell line (15p-1), the somatic support cell found in the testis seminiferous tubules (Rassoulzadegan et al., 1993). Anti-ZFR antibodies detected a 150 kDa band present only in the nuclear fractions (Fig. 6, arrow, lanes 1–4). In addition, several lower molecular weight bands were found in both the nuclear and cytoplasmic fractions. To determine which band represented ZFR, the same blot was stripped and reprobed with anti-ZFR antibodies that had been preabsorbed with the MBP-ZFR fusion protein. This pre-treatment specifically blocked detection of the 150 kDa band in both the testis and Sertoli nuclear fractions (lanes 5–8).

The size of the ZFR protein was also examined by performing coupled in vitro transcription and translation from the *Zfr* composite cDNA. The *Zfr* cDNA predicts a size of 114 kDa, yet a protein product of 150 kDa was detected by ^{35}S-methionine autoradiography. Western blot analysis demonstrated that the product co-migrates with the 150 kDa band from 15p-1 nuclei (lanes 9–11). These data suggest that ZFR migrates aberrantly in SDS–PAGE.

If the deletion in cDNA *Zfr.2* represents an alternatively spliced RNA form, then translation of this variant would frameshift and terminate at the deletion site (amino acid #858), producing a 95.3 kDa protein. A specific 95.3 kDa ZFR protein was not detected by the western blot and antibody preabsorption experiments described above.

3.7. Localization of ZFR protein in the testis

Immunohistochemistry was performed on adult testis to determine the ZFR protein expression profile (Fig. 7). Carnoy's fixed testis sections incubated with preimmune serum displayed no background staining (Fig. 7H). Sections treated with anti-ZFR antibodies displayed a pronounced immunopositive stain in the nuclei of pachytene spermatocytes (Fig. 7A–F). Within pachytene spermatocyte nuclei, ZFR co-localizes with the chromatin and appears to be absent from the interchromosomal spaces (Fig. 7F). As these meiotic prophase cells progress from the earliest stages of pachytene to the mid and late stages, the nuclei become enlarged and the chromatin becomes increasingly visible. Throughout the course of the pachytene stage, the pattern of ZFR staining reflects the chromatin distribution.

To test whether ZFR was specifically localized to the principal structural component of pachytene spermatocytes, the synaptonemal complex (SC), co-immunofluorescence was performed on spread spermatocytes using human anti-SC auto-antibodies (Haaf et al., 1989) and anti-ZFR antibodies (Fig. 7G). Compared with the distinct anti-SC staining, ZFR signal showed a broader distribution in the nucleus. This

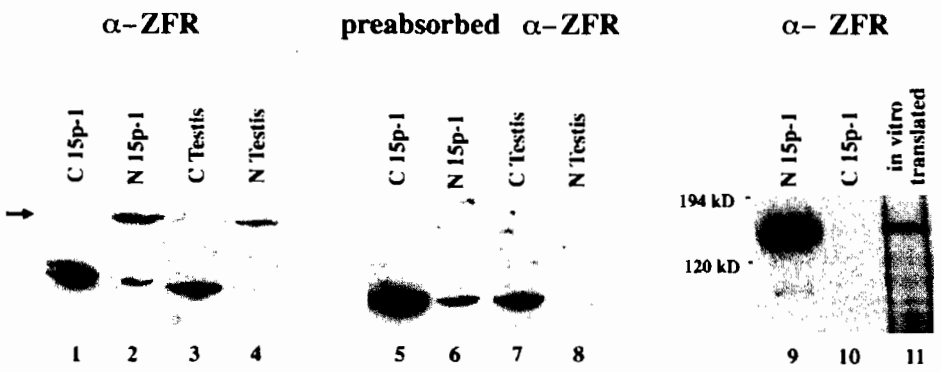

Fig. 6. Western blot analysis of the ZFR protein using anti-ZFR affinity purified antibody. Protein extracts from testis (lanes 3, 4, 7, and 8) or the Sertoli cell line 15p-1 (lanes 1, 2, 5, 6, 9, and 10) were fractionated and electrophoretically separated on an 8% SDS–polyacrylamide gel. C = cytoplasmic fraction; N = nuclear fraction. The blot containing lanes 1–4 was stripped and reprobed with anti-ZFR antibody that had been preabsorbed with MBP-ZFR fusion protein (lanes 5–8). A second blot (lanes 9–11) illustrates the strong 150 kDa band signal in the nucleus (lane 9). The band co-migrates with the specific product generated from coupled in vitro transcription and translation of full-length *Zfr* cDNA in rabbit reticulocyte extract (lane 11).

observation suggests that ZFR localization in pachytene cells is not restricted to the synaptonemal complex.

During the brief diplotene stage of prophase, the ZFR signal remains strong. At metaphase, when the nuclear envelope breaks down and the chromosomes congress to the metaphase plate, ZFR becomes distributed throughout the cytoplasm (Fig. 7C and E). In contrast to the observation in pachytene cells, ZFR staining is now excluded from the prometaphase and metaphase chromosomes. Inspection of these cells by immunofluorescence showed no overlap between ZFR staining and the chromosomes (data not shown), although slightly pronounced ZFR staining can be seen at the periphery of the metaphase chromosomes (Fig. 7E).

In germ cells, ZFR appears to be upregulated for the pachytene spermatocyte stage and downregulated before spermatids elongate. The spermatogonial cells and early meiotic prophase cells, such as leptotene and zygotene (Fig. 7E), display either undetectable or much reduced levels of ZFR. After meiosis, a weak signal remains in the earliest round spermatids (data not shown). ZFR immunostain declines and disappears as the early haploid cells develop into late round and elongating spermatids (Fig. 7B–F). Because *Prm1* is first transcribed in late round spermatids, ZFR is unlikely to interact with *Prm1* mRNA in vivo (see Section 4).

Prominent ZFR expression was also observed in the supporting somatic Sertoli cells. Staining was found throughout the nucleus in a punctate pattern except at the nucleoli (Fig. 7B and F). The ZFR signal in Sertoli cells is especially prominent compared with the signal in other testis somatic cells. Staining in the interstitial Leydig cells and seminiferous epithelial myoid cells is sparse and variable, ranging from undetectable to weak.

To test whether the staining pattern observed in the testis is due specifically to the anti-ZFR antibodies, an aliquot of the antibody preparation was preincubated with MBP-ZFR fusion protein prior to immunohistochemistry. This treatment blocked the anti-ZFR antibodies and abolished the immunostaining (data not shown). In addition, immunohistochemistry with an anti-MBP antibody revealed no signal (data not shown).

In summary, ZFR is detected at highest levels in pachytene spermatocytes, where it is chromosome associated, and in Sertoli cells. ZFR is expressed at either very low levels, or is not detected at all, in pre- and post-meiotic cells, and in other somatic cells in the testis.

3.8. *Localization of ZFR in the ovary*

To determine whether ZFR is expressed in the homologous cell types in the female gonad, immunohistochemistry and immunofluorescence was performed on adult mouse ovary sections. Immunopositive signal was most apparent in the ovarian follicles (Fig. 8A–C). In the oocyte, staining was localized within the nucleus and was completely absent from the cytoplasm (Fig. 8B and C). Granulosa cells, in follicles ranging from the primary to the antral stage, displayed a strong signal. Signal was also observed in the surrounding thecal and stromal cells at markedly diminished levels (Fig. 8A). A subset of the cells in the corpus luteum were also immunopositive for ZFR, whereas others failed to stain (Fig. 8B). As in the testis, ZFR expression is most prominent in prophase I germ cells and the support cells.

By confocal microscopy, ZFR protein appeared to be distributed within the oocyte nucleus as a fibrillar mesh (Fig. 8F). ZFR staining appeared to overlap with the DNA signal (Fig. 8G), suggesting that ZFR co-localizes with oocyte chromosomes.

A mitotically dividing granulosa cell, captured at telophase, shows segregated chromosomes devoid of ZFR signal (Fig. 8E). ZFR protein is dispersed through-

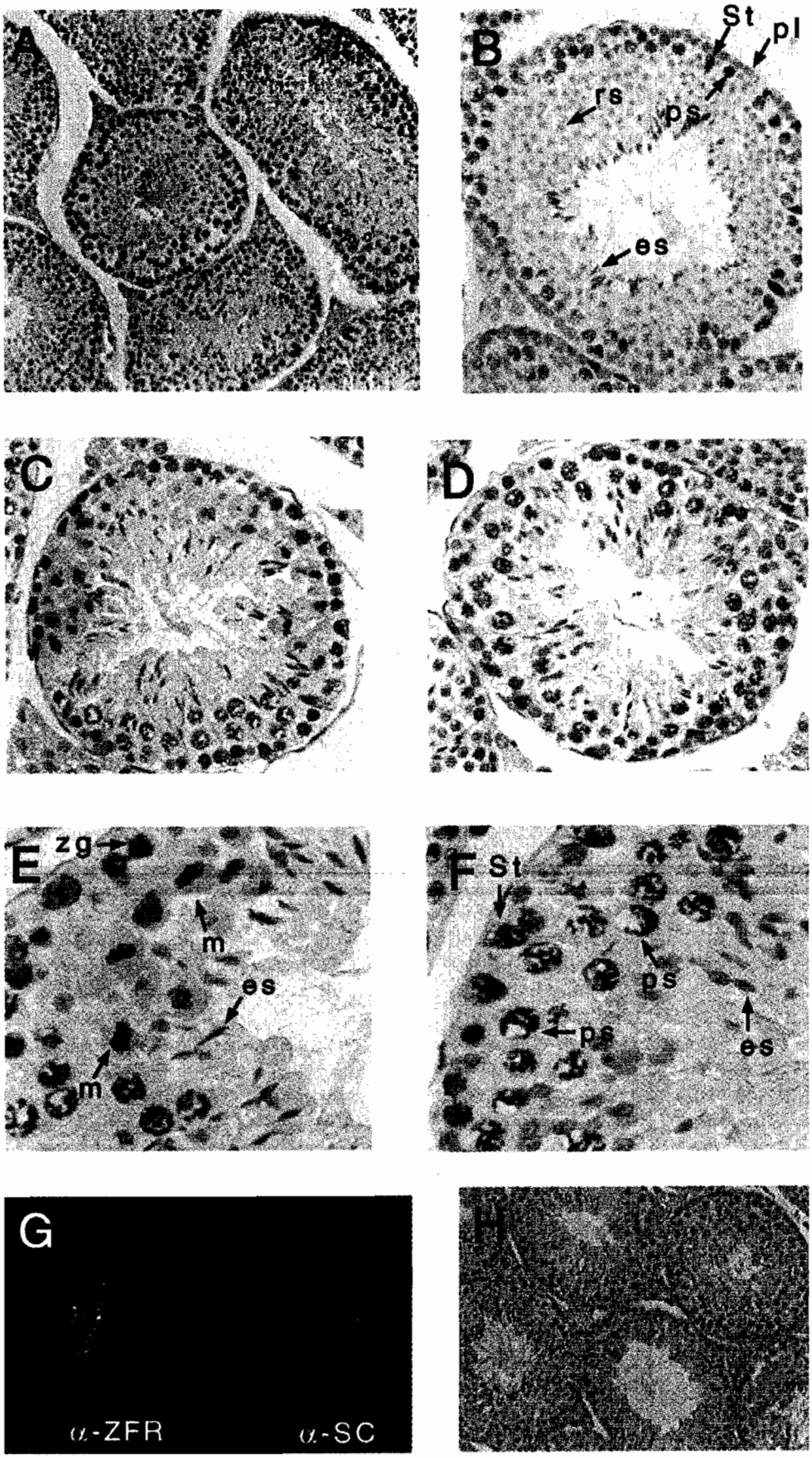
A
B
St
pl
rs
ps
es
C
D
E
zg
m
es
m
F
St
ps
ps
es
G
α-ZFR
α-SC
H

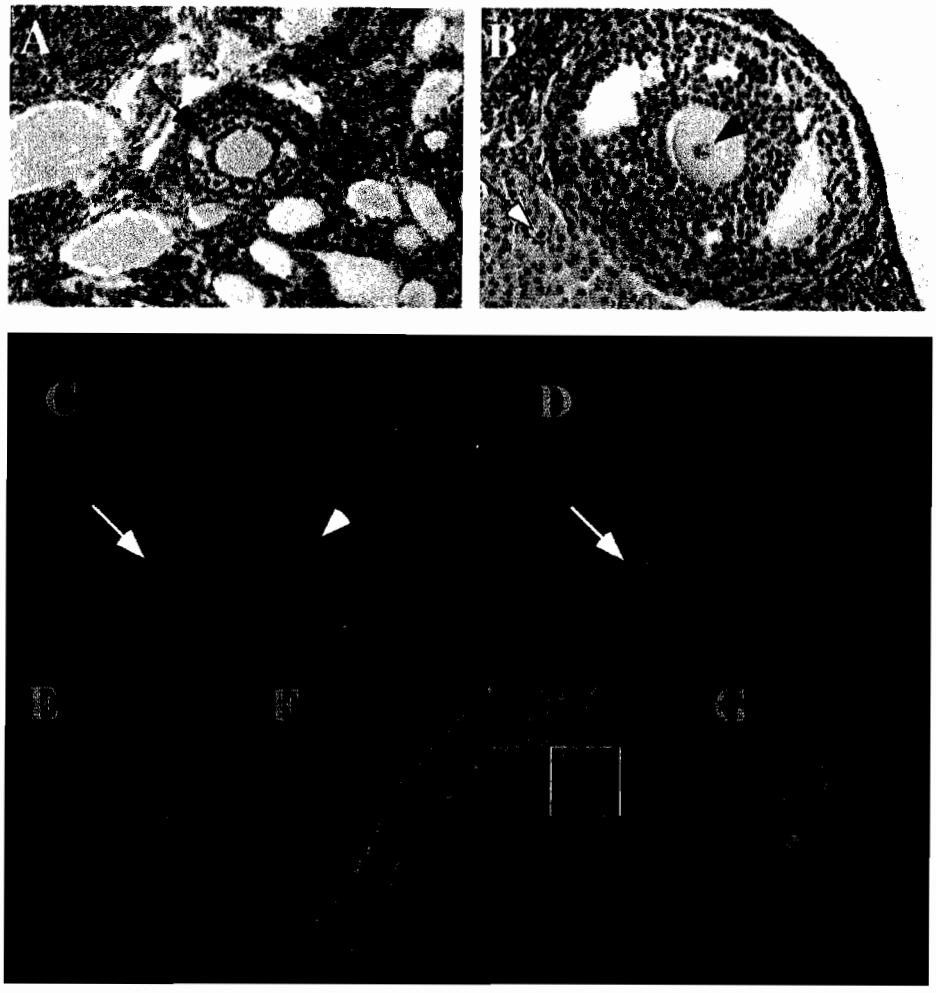

Fig. 8. Localization of ZFR in the adult mouse ovary by immunohistochemistry and immunofluorescence. (A) ZFR immunostaining in the granulosa cells of a follicle (arrow).The oocyte nucleus lies outside the plane of section. (B) Discrete, localized ZFR immunostaining in the oocyte nucleus (arrowhead). Signal is also strong in granulosa cells and a population of corpus lutein cells (open arrow in lower left corner). (C, D, E, F) Confocal imaging of an ovarian follicle displays the fluorescein-labeled anti-ZFR immunolocalization (green), the propidium iodide counterstain signal (red), and the overlap in the signals (yellow). ZFR staining is noticeably absent in a cluster of connective tissue cells (arrows in C and D). (E) Higher magnification of a mitotically dividing granulosa cell shown boxed in (F). (G) Closer view of the overlap of anti-ZFR and propidium iodide signal in another oocyte nucleus.

out the cytoplasm. This change in localization during mitosis is similar to the change in localization observed during meiotic metaphase in male germ cells.

3.9. Nucleic acid filter binding assay

Because ZFR is unlikely to bind *Prm1* in vivo, northwestern and southwestern assays were performed with bacterially expressed ZFR protein to assess its capacity to bind nucleic acid substrates other than *Prm1* mRNA. Oligohistidine-tagged ZFR fusion proteins were expressed from pET15b plasmids carrying the composite *Zfr* cDNA, which contains the full open reading frame, or cDNA *Zfr.1*, which encodes the second and third zinc fingers and the ZRA regions (amino acids 340–1052). Analysis of the induced extracts by SDS–PAGE Coomassie Blue staining and western blotting showed strong expression of the His_6-ZFR.1 protein (Fig. 9A,

Fig. 7. Localization of ZFR within the mouse testis. Immunohistochemistry was performed with affinity-purified anti-MBP-ZFR antibodies. Sections were counterstained with hematoxylin. (A) Seminiferous tubules, 200× magnification. (B) Stage VIII tubule, 400× magnification, shows Sertoli cells (St), pre-leptotene cells (pl), pachytene spermatocytes (ps), round spermatids (rs) and elongated spermatids (es). (C) Stage XII tubule, 400× magnification, shows spermatocytes in metaphase. (D) Chromosomal association of ZFR in pachytene spermatocytes of Stage IX tubule, 400× magnification. (E) 800× magnification of metaphase cells (m) and zygotene cells (zg) of Stage XII tubule. (F) 800× magnification of pachytene spermatocytes and Sertoli cells in Stage IX tubule. (G) Confocal image of fluorescein-labeled anti-ZFR antibody staining and Texas Red-labeled human anti-synaptonemal complex antibody staining in spread spermatocytes. (H) Immunohistochemistry with pre-immune serum shows no staining, 200× magnification.

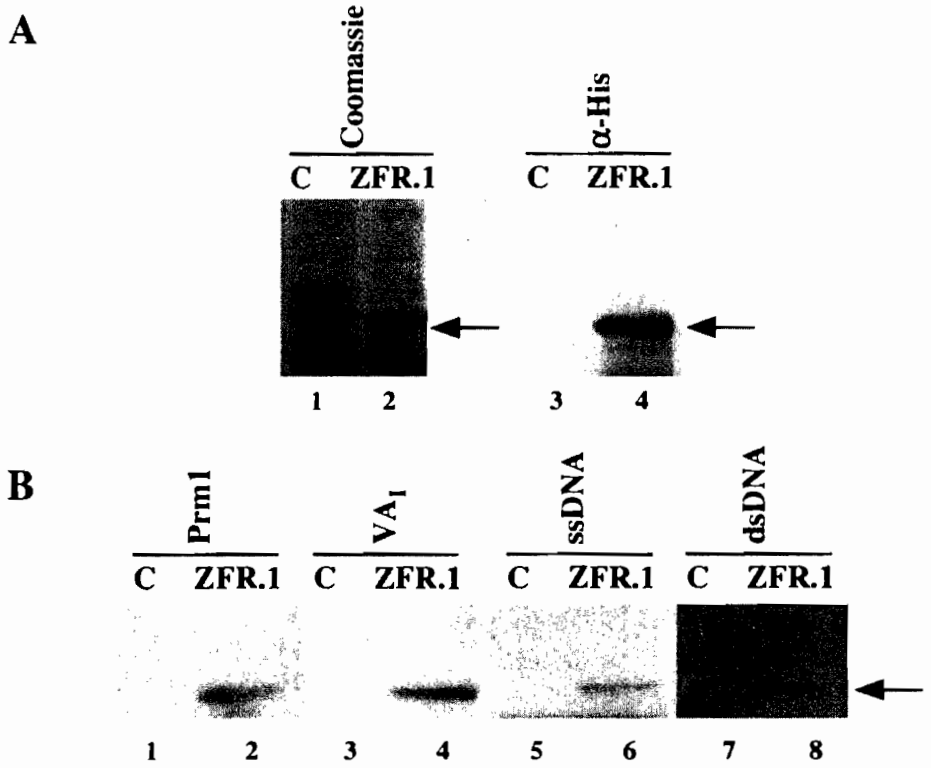

Fig. 9. (A) SDS–PAGE Coomassie Blue staining (lanes 1 and 2) and anti-His antibody western blots (lanes 3 and 4) of induced crude bacterial extracts expressing pET15b (lanes 1 and 3) or pET15b-ZFR.1 (lanes 2 and 4). Arrows point to the 82 kDa His_6-ZFR.1 fusion protein in the pET15b-ZFR.1 extracts. (B) RNA and DNA binding assays. PVDF membranes containing induced pET15b extracts [control (C); lanes 1, 3, 5, and 7]; or induced pET15b-ZFR.1 extracts (lanes 2, 4, 6, and 8) were probed with radiolabeled *Prm1* RNA (1 and 2), VA RNA_I (3 and 4), heat denatured DNA (5 and 6), and renatured DNA (7 and 8). All probes bound the His_6-ZFR.1 protein (arrow). *Spnr* cDNA was used as a non-biologically relevant sequence to generate the DNA probes.

lanes 2 and 4, arrows) and weaker expression of the His_6-ZFR full length protein (data not shown). Because of this observation, and because ZFR.1 had previously demonstrated RNA binding in the cDNA expression library screen, the His_6-ZFR.1 crude protein extracts were used for subsequent binding assays (Fig. 9A and B, even lanes). As a control, crude protein extracts from induced cultures bearing the pET15b vector, which without an insert encodes a 4.9 kDa fusion protein, were included in each assay (Fig. 9A and B, odd lanes). PVDF membranes containing the protein extracts were subjected to 8 M urea denaturation followed by slow renaturation. Membrane strips of a single blot were incubated with radiolabeled heat-denatured *Prm1* 3′UTR RNA (Fig. 9B, lanes 1 and 2), renatured adenovirus virus associated (VA) RNA_I (lanes 3 and 4), denatured DNA (lanes 5 and 6) and double-stranded DNA (lanes 7 and 8). Westerns with anti-His antibodies confirmed the expression and marked the migration of the 82 kDa His_6ZFR.1 fusion protein (Fig. 9A, lane 4). In each binding assay, a band specific to the pET15b-ZFR.1 extract that co-migrated with the 82 kDa His_6ZFR.1 fusion protein bound the radiolabeled nucleic acid. Thus the His_6ZFR.1 fusion protein, in addition to binding *Prm1*, displayed affinity for both forms of DNA and for VA RNA_I, a highly structured RNA containing duplexed regions.

4. Discussion

4.1. *Identification of* Zfr *in an RNA-binding screen*

Zfr was cloned in a northwestern-like screen designed to identify RNA binding proteins that exhibited a preference for *Prm1* 3′UTR RNA. ZFR most likely does not function, however, in the translational repression of *Prm1* in vivo. ZFR protein is not detectable in late-stage round spermatids which synthesize *Prm1* RNA. Furthermore, the ZFR protein, which possesses two possible nuclear localization signals, was detected by western blotting in nuclear fractions only and not in cytoplasmic extracts. In contrast, *Prm1* message is stored and translationally repressed in the cytoplasm of late round and elongating spermatids. It is possible that the cloning of two independent *Zfr* cDNAs from the screen was fortuitous. Alternatively, the expressed *Zfr* clones may have had a stronger affinity for RNA than the numerous other zinc finger proteins encoded in the testis library, and favored the *Prm1* 3′ UTR probe for its

structural elements. The 3′UTR of *Prm1* contains two repeat sequences capable of forming a stable stem-loop structure with an imperfect, intervening antisense copy of the repeat (Lee et al., 1996).

A striking outcome of the library screen was the cloning of three genes all sharing a common novel domain. *Zfr*, *Spnr* (Schumacher et al., 1995b) and the mouse homolog of *NF90* (unpublished data), all encode the ZRA1 and ZRA2 regions in addition to recognizable nucleic acid binding motifs (i.e. three zinc fingers for *Zfr* and two dsRNA binding motifs each for *Spnr* and mouse *NF90*). It is interesting to consider that the ZRA domains may have modulated the specificity or strength of their binding to the *Prm1* RNA probe. The discovery of *Zfr* demonstrates for the first time that the domains are evolutionarily conserved not only within a set of similarly organized dsRNA binding proteins, but also separately in the context of a different nucleic acid binding domain.

4.2. Zinc fingers in ZFR

The three zinc fingers in ZFR generally match the zinc finger motif consensus, $Y/FXCX_{2,4}CX_3X_5\underline{L}X_2HX_{3-5}H$ (Pieler and Bellefroid, 1994). However, certain features of the fingers suggest that the properties of ZFR may differ from those of traditional zinc finger proteins. Protein database searches display significant matches between the zinc fingers in ZFR and those in the *X. laevis* RNA-binding zinc finger protein dsRBP-ZFa. Binding studies using expressed dsRBP-ZFa protein have demonstrated its particularly strong affinity for double-stranded RNA molecules and DNA:RNA hybrids. The last four fingers in dsRBP-ZFa and first two fingers in ZFR have modifications at two conserved sites within the 12 residue stretch between the cysteines and histidines. Instead of having an aromatic residue at the fourth position and an aliphatic residue at the tenth position (denoted by and $\underline{L}$ respectively in the consensus above), the positions of these residues are reversed. Additionally, these fingers have a tyrosine substitution for the phenylalanine (Finerty and Bass, 1997). Furthermore, the fingers in ZFR and dsRBP-ZFa have long interhistidine distances of five residues instead of the more common spacing of three to four residues. Four of the five interhistidine residues in ZFR finger 2 are identical to those in dsRBP-ZFa fingers 5 and 6. Studies of DNA-binding zinc fingers have shown that the histidines contribute to a short alpha-helical element that makes contacts with the major groove of DNA(Klug and Schwabe, 1995). The conserved residues in the fingers of ZFR might be important for binding DNA helices or RNA A-form helices.

The ZFR fingers are not directly linked but are instead differentially spaced from each other. Most zinc finger proteins have well conserved linkers of seven amino acids which cluster the fingers and contribute to their conformation and nucleic acid binding (Schuh et al., 1986; Klug and Rhodes, 1987). The widely spaced fingers of ZFR lack this linker sequence. It has been suggested that widely spaced fingers may allow the protein greater versatility in its binding specificity, strength, and span (Reuter et al., 1990; Fasano et al., 1991). Some proteins with isolated and widely spaced zinc finger motifs have non-classical targets: *Drosophila* protein PEP is thought to bind nascent RNA; *X. laevis* dsRBP-ZFa binds dsRNA and DNA:RNA hybrids in vitro; and *Drosophila* Suvar(3)7 plays a role in defining heterochromatin and euchromatin boundaries (Amero et al., 1993; Cléard et al., 1995; Finerty and Bass, 1997).

4.3. Conservation of a novel protein domain

ZFR contains a domain that has been conserved in a collection of frog, mouse, and human dsRNA binding motif-containing proteins. The extent of conservation is striking: 65% amino acid identity or 75% amino acid similarity when conservative substitutions are considered. Two proteins containing the conserved ZRA regions, 4F.1 and 4F.2, were cloned from a *Xenopus laevis* ovary cDNA expression library screened with labeled double-stranded RNA, a screen similar to the testis cDNA expression library screen described above (Bass et al., 1994).

SPNR protein has been shown to bind RNA, but not DNA, in vitro by northwestern assays. Its localization to a cytoplasmic microtubule array in spermatids suggests it could mediate RNA transport or translational activation (Schumacher et al., 1995b). A fusion protein containing *Xenopus* 4F.1 sequence was shown to bind dsRNA and, to a lesser extent, RNA:DNA hybrids by electrophoretic mobility shift assays. In vivo substrates for 4F.1 and 4F.2 have not been reported, although possibilities include interactions with double-stranded RNA structure at splice sites or with RNA:DNA hybrids at active transcription and replication sites (Bass et al., 1994).

In contrast, NF90, the human homolog of *Xenopus* 4F.1, and NF45 were identified via biochemical purification as members of the nuclear factor of activated T-cells (NF-AT) transcription factor complex for the interleukin-2 promoter (Kao et al., 1994). Via a separate approach, NF90 and NF45 were co-purified, as a dimer, with DNA-dependent kinase, a serine-threonine kinase required for V(D)J recombination and DNA double-strand break repair (Ting et al., 1998). Recombinant NF90 can promote complex formation of the DNA-dependent kinase catalytic subunit with its DNA binding subunit and DNA substrate. NF45 interacts with this complex, but only when associated with NF90 (Ting et al., 1998). The physical association between NF90 and NF45, and the observation that the NF45 amino

acid sequence contains the ZRA2 region and no recognizable nucleic acid binding motif, suggests the possibility that the region could function as a protein–protein interaction domain. The function of the dsRNA binding domains in NF90 in the context of these activities has not been tested.

4.4. Expression of ZFR in homologous cell types in the testis and ovary

ZFR is expressed in a subset of germ and somatic cells in the testis and ovary. An examination of male germ cells at the spermatogonial stage and the early meiotic preleptotene, leptotene and zygotene stages revealed a low or undetectable level of ZFR antibody signal. In contrast, a strong ZFR signal was seen specifically at the pachytene stage of meiosis that continued until the early round spermatid stage. Downregulation of ZFR expression probably takes place in these spermatids since ZFR protein is absent in elongating spermatids and spermatozoa.

Throughout pachytene, the chromatin is visibly condensed. During mid to late pachytene, the tight associations between the chromosomes and the nuclear envelope, to which they are attached, generate visible interchromosomal spaces in the nucleus. The size of spermatocyte nuclei, and the prominence of the pachytene chromosomes, conferred the ability to observe ZFR protein's association with the chromosomes by immunohistochemistry. ZFR staining was absent from the interchromosomal spaces of pachytene nuclei. ZFR appeared to associate with the chromosomes and change accordingly as the chromatin configuration changed.

Immunohistochemistry results revealed that ZFR protein expression, although particularly strong in spermatocytes, is not meiosis-specific. The somatic Sertoli cell also displayed strong nuclear staining. The homologous cell types in the ovary, the oocytes and their surrounding follicle cells, were immunopositive. ZFR could have the same biochemical function in germ cells and somatic cells. Alternatively, ZFR could have a specialized function in the meiotic process that has been adapted from its more general function in somatic cells.

The chromosomal localization of ZFR is lost at metaphase during both meiosis and mitosis. This transition might be regulated or just be the consequence of nuclear envelope breakdown. Alternatively, the displacement of ZFR could be required for nuclear envelope breakdown. Studies of ZFR protein from metaphase-arrested tissue culture cells might reveal modifications to ZFR protein such as phosphorylation.

After meiosis, the chromatin organization is altered again in the developing spermatids as the transition proteins and protamines replace the histones for greater DNA compaction. The absence of ZFR in these cells suggest that its retention might be incompatible with chromatin compaction. Alternatively, ZFR expression might decrease because it is not required at this stage of germ cell development.

4.5. Putative targets and functions for ZFR

Nucleic acid binding assays revealed that ZFR can bind both RNA and DNA molecules in vitro. We do not know whether ZFR possesses different affinities for the various substrates nor whether ZFR functionally interacts with DNA or RNA in vivo. The apparent chromosomal localization of ZFR is consistent with either DNA- or RNA-binding activities. Possible functions for ZFR include roles in DNA repair and chromosome organization. In a manner analogous to NF90 and NF45, ZFR could, via its ZRA regions, potentially complex with DNA binding proteins such as DNA-PK. Alternatively, ZFR could associate with chromatin directly, where it could have a role in configuring chromatin for active or inactive transcriptional states or in organizing changes in chromosome condensation or movement.

Additionally, ZFR could function in transcription complex formation and activation. The amino terminal end of ZFR contains polyglutamine and polyalanine repeats, a feature found in bona fide transcriptional activators and in many *Drosophila* developmental genes. One piece of evidence that suggests ZFR is not a transcriptional activator comes from preliminary tests of ZFR in a yeast two-hybrid system. Expression of full-length ZFR fused to the yeast GAL4 DNA binding domain does not activate expression of yeast reporter genes (data not shown).

ZFR might interact with nascent RNA at the site of transcription or be part of a complex for RNA processing. Studies of interphase nuclei suggest that transcription occurs at the base of chromosomal loops at points of attachment to the nuclear matrix (Cook, 1994). This type of localization has been observed for RNA polymerase and hnRNP complexes by biochemical fractionation and immunolocalization studies (Carter et al., 1991,1993; Fackelmayer et al., 1994). Preliminary experiments suggest that ZFR protein co-purifies with nuclear matrix fractions (unpublished observations). Results from the two-hybrid screen will potentially identify ZFR-interacting proteins and might suggest the pathway in which ZFR functions in vivo.

The presence of *Zfr* in humans, worms and flies indicates that *Zfr* has been evolutionarily conserved. *Zfr* likely functions in germ cell development, and perhaps in other developmental pathways, in these organisms as well as in the mouse. Surprisingly, mutations in the *Drosophila* and *C. elegans* homologs have not been reported. Analysis of *Zfr* mutations in any of these model organisms would contribute to the understanding of its function. We have recently generated a

null allele for *Zfr* in the mouse via targeted mutagenesis (unpublished). Our preliminary data suggest that *Zfr* is an essential gene.

Acknowledgements

We thank Dr Thomas Haaf for kindly providing the human anti-synaptonemal complex sera, Glen McDonald for assistance with confocal microscopy, and Todd Berard and the Department of Pharmacology and Molecular Pharmacology Facility for oligonucleotide synthesis and DNA sequencing. This work was supported by grants from the National Institutes of Health to REB (HD27215 and HD95003) and CD (GM46883).

References

Amero, S.A., Matunis, M.J., Matunis, E.L., Hockensmith, J.W., Raychaudhuri, G., Beyer, A.L., 1993. A unique ribonucleoprotein complex assembles preferentially on ecdysone-responsive sites in Drosophila melanogaster. Mol. Cell Biol. 13, 5323–5330.

Bass, B.L., Hurst, S.R., Singer, J.D., 1994. Binding properties of newly identified Xenopus proteins containing dsRNA-binding motifs. Curr. Biol. 4, 301–314.

Braun, R.E., Peschon, J.J., Behringer, R.R., Brinster, R.L., Palmiter, R.D., 1989. Protamine 3′-untranslated sequences regulate temporal translational control and subcellular localization of growth hormone in spermatids of transgenic mice. Genes Dev. 3, 793–802.

Brendel, V., Bucher, P., Nourbakhsh, I.R., Blaisdell, B.E., Karlin, S., 1992. Methods and algorithms for statistical analysis of protein sequences. Proc. Natl. Acad. Sci. USA 89, 2002–2006.

Carter, K.C., Bowman, D., Carrington, W., Fogarty, K., McNeil, J.A., Fay, F.S., Lawrence, J.B., 1993. A three-dimensional view of precursor messenger RNA metabolism within the mammalian nucleus (see comments). Science 259, 1330–1335.

Carter, K.C., Taneja, K.L., Lawrence, J.B., 1991. Discrete nuclear domains of poly(A) RNA and their relationship to the functional organization of the nucleus. J. Cell Biol. 115, 1191–1202.

Céard, F., Matsarskaia, M., Spierer, P., 1995. The modifier of position-effect variegation Suvar(3)7 of Drosophila: there are two alternative transcripts and seven scattered zinc fingers each preceded by a tryptophan box [published erratum appears in Nucleic Acids Res., 1995. 23 (18), 3804]. Nucleic Acids Res. 23, 796–802.

Cook, P.R., 1994. RNA polymerase: structural determinant of the chromatin loop and the chromosome. Bioessays 16, 425–430.

Edelhoff, S., Ayer, D.E., Zervos, A.S., Steingrímsson, E., Jenkins, N.A., Copeland, N.G., Eisenman, R.N., Brent, R., Disteche, C.M., 1994. Mapping of two genes encoding members of a distinct subfamily of MAX interacting proteins: MAD to human chromosome 2 and mouse chromosome 6 and MXI1 to human chromosome 10 and mouse chromosome 19. Oncogene 9, 665–668.

Epplen, C., Epplen, J.T., 1994. Expression of (cac)n/(gtg)n simple repetitive sequences in mRNA of human lymphocytes. Hum Genet. 93, 35–41.

Fackelmayer, F.O., Dahm, K., Renz, A., Ramsperger, U., Richter, A., 1994. Nucleic-acid-binding properties of hnRNP-U/SAF-A, a nuclear-matrix protein which binds DNA and RNA in vivo and in vitro. Eur. J. Biochem. 221, 749–757.

Fasano, L., Roder, L., Coré, N., Alexandre, E., Vola, C., Jacq, B., Kerridge, S., 1991. The gene teashirt is required for the development of Drosophila embryonic trunk segments and encodes a protein with widely spaced zinc finger motifs. Cell 64, 63–79.

Finerty Jr, P.J., Bass, B.L., 1997. A Xenopus zinc finger protein that specifically binds dsRNA and RNA-DNA hybrids. J. Mol. Biol. 271, 195–208.

Haaf, T., Machens, A., Schmid, M., 1989. Immunocytogenetics. II. Human autoantibodies to synaptonemal complexes. Cytogenet. Cell Genet. 50, 6–13.

Kao, P.N., Chen, L., Brock, G., Ng, J., Kenny, J., Smith, A.J., Corthésy, B., 1994. Cloning and expression of cyclosporin A- and FK506-sensitive nuclear factor of activated T-cells: NF45 and NF90. J. Biol. Chem. 269, 20691–20699.

Klug, A., Rhodes, D., 1987. Zinc fingers: a novel protein fold for nucleic acid recognition. Cold Spring Harb. Symp. Quant. Biol. 52, 473–482.

Klug, A., Schwabe, J.W., 1995. Protein motifs 5. Zinc fingers. Faseb. J. 9, 597–604.

Lee, K., Fajardo, M.A., Braun, R.E., 1996. A testis cytoplasmic RNA-binding protein that has the properties of a translational repressor. Mol. Cell Biol. 16, 3023–3034.

Pieler, T., Bellefroid, E., 1994. Perspectives on zinc finger protein function and evolution — an update. Mol. Biol. Rep. 20, 1–8.

Rassoulzadegan, M., Paquis Flucklinger, V., Bertino, B., Sage, J., Jasin, M., Miyagawa, K., van Heyningen, V., Besmer, P., Cuzin, F., 1993. Transmeiotic differentiation of male germ cells in culture. Cell 75, 997–1006.

Reuter, G., Giarre, M., Farah, J., Gausz, J., Spierer, A., Spierer, P., 1990. Dependence of position-effect variegation in Drosophila on dose of a gene encoding an unusual zinc-finger protein. Nature 344, 219–223.

Robbins, J., Dilworth, S.M., Laskey, R.A., Dingwall, C., 1991. Two interdependent basic domains in nucleoplasmin nuclear targeting sequence: identification of a class of bipartite nuclear targeting sequence. Cell 64, 615–623.

Sambrook, J., Fritsch, E.F., Maniatis, T., 1989. Molecular Cloning, A Lab Manual. 2nd edition Cold Spring Harbor Press, Cold Spring Harbor, NY.

Schuh, R., Aicher, W., Gaul, U., Coté, S., Preiss, A., Maier, D., Seifert, E., Nauber, U., Schroder, C., Kemler, R., 1986. A conserved family of nuclear proteins containing structural elements of the finger protein encoded by Kruppel, a Drosophila segmentation gene. Cell 47, 1025–1032.

Schumacher, J.M., Lee, K., Edelhoff, S., Braun, R.E., 1995a. Distribution of TENR, an RNA binding protein, in a lattice-like network within the spermatid nucleus in the mouse. Biol. Reprod. 52, 1274–1283.

Schumacher, J.M., Lee, K., Edelhoff, S., Braun, R.E., 1995b. SPNR, a murine RNA-binding protein that is localized to cytoplasmic microtubules. J. Cell Biol. 129, 1023–1032.

St Johnston, D., Brown, N.H., Gall, J.G., Jantsch, M., 1992. A conserved double-stranded RNA-binding domain.. Proc. Natl. Acad. Sci. USA 89, 10979–10983.

Ting, N.S., Kao, P.N., Chan, D.W., Lintott, L.G., Lees Miller, S.P., 1998. DNA-dependent protein kinase interacts with antigen receptor response element binding proteins NF90 and NF45. J. Biol. Chem. 273, 2136–2145.